Contents list available at IJRED website

International Journal of Renewable Energy Development

Journal homepage: https://ijred.undip.ac.id

Research Article

Performance Evaluation of An Electrolyte-Supported Intermediate-Temperature Solid Oxide Fuel Cell (IT-SOFC) with Low-Cost Materials

Fauzi Yusupandi[a,b], Hary Devianto[a*], Pramujo Widiatmoko[a], Isdiriayani Nurdin[a], Sung Pil Yoon[c], Tae-Hoon Lim[c], Aditya Farhan Arif[d]

[a]*Department of Chemical Engineering, Faculty of Industrial Technology, Institut Teknologi Bandung, Jl. Ganesha No. 10, Bandung 40132, Indonesia*

[b]*Department of Chemical Engineering, Institut Teknologi Sumatera, Jl. Terusan Ryacudu, Way Huwi, Kec. Jati Agung, Lampung Selatan 35365, Indonesia*

[c]*Center for Hydrogen-Fuel Cell Research, Korea Institute of Science and Technology (KIST), 5, Hwarangro 14-gil, Seongbuk-gu, Seoul, South Korea*

[d]*Department of New Investment, PT Rekayasa Industri, Jl. Kalibata Timur I No. 36, Jakarta 12740, Indonesia*

Abstract. Intermediate temperature solid oxide fuel cell (IT-SOFC) provides economic and technical advantages over the conventional SOFC because of the wider material use, lower fabrication cost and longer lifetime of the cell components. In this work, we fabricated electrolyte-supported IT-SOFC using low-cost materials such as calcia-stabilized zirconia (CSZ) electrolyte fabricated by dry-pressing, NiO-CSZ anode and Ca3Co1.9Zn0.1O6 (CCZO) cathode produced through brush coating technique. According to the XRD result, the monoclinic phase dominated over the cubic phase, and the relative density of the electrolyte was low but the hardness of the CSZ electrolyte was close to the hardness of commercial 8YSZ electrolyte. The performance of the single cell was performed with hydrogen ambient air. An open-circuit voltage (OCV) of 0.43, 0.46, and 0.45 V and a maximum power density of 0.14, 0.50, and 1.00 mW/cm2 were achieved at the operating temperature of 600, 700, and 800 °C, respectively. The ohmic resistance of the cell at 700 and 800 °C achieved 81.5 and 33.00 Ω, respectively due to the contribution of thick electrolyte and Cr poisoning in electrodes and electrolyte.

Keywords: IT-SOFC; calcia-stabilized zirconia; electrolyte-supported; operating temperature; single cell

Received: 17th May 2021; Revised: 8th July 2022; Accepted: 15th July 2022; Available online: 21st July 2022

1. Introduction

Solid oxide fuel cell (SOFC) offers high electrical efficiency (up to 70%), zero or low emissions of pollutants, modularity, quiet operation, wide range of fuel options and capability to operate in hybrid power generating system (Irshad *et al*., 2016; Fleischhauer *et al*., 2015; Abdalla *et al*., 2018). SOFC is commonly performed at 850 – 1,000 °C called high-temperature SOFC (HT-SOFC). However, the fabrication and operation cost of HT-SOFC have remained high due to high heat and complex materials. The development of intermediate-temperature SOFC (IT-SOFC) is paramount to accelerate the wide application of SOFC since IT-SOFC operates below 800 °C to reduce heat requirement and material cost (Fragiacomo *et al*., 2020; Shi *et al*., 2020).

The tubular and planar SOFC are common designs in SOFC systems. Compared to tubular, a planar shape has lower production cost and higher power density (Timurkutluk *et al*., 2016). A planar SOFC is classified into two configurations: an electrode-supported and electrolyte-supported cell. Electrode-supported cells, consisting of anode and cathode-supported, can operate at 600 – 800 °C because of thin electrolytes. However, the configurations have several disadvantages such as a limitation of mass transport, potential anode re-oxidation for anode-supported and low conductivity for cathode-supported. An electrolyte-supported SOFC is a conventional design of SOFC cell using thick electrolyte to support thin electrodes on both surfaces. The minimum thickness of electrolyte-supported configuration is ~150 µm to avoid cracks during the sealing (Chelmehsara & Mahmoudimehr, 2018). The advantages of this design are robust structure and resistant to anode re-oxidation resulting in cell degradation. However, the electrolyte-supported

* Corresponding author:
Email: hardev@che.itb.ac.id (H.Devianto)

https://doi.org/10.14710/ijred.2022.46735
ISSN: 2252-4940/© 2022.The Author(s). Published by CBIORE

configuration requires high operating temperature to reduce ohmic resistance (Singhal & Kendall, 2003).

Yttria-stabilized zirconia (YSZ) has been utilized as an electrolyte in SOFCs for a long time owing to chemical fitness with cermet electrodes, excellent thermal stability, and strong ionic conductivity. Nevertheless, price of yttria is exorbitant and low resources worldwide (U.S. Geological Survey, 2019; Zhang *et al*., 2017). Calcia (CaO) can be a promising alternative stabilizer to zirconia owing to its economical price and abundant reserve. In contrast to YSZ, which reverts to monoclinic phase at low temperatures, the cubic structure of calcia-stabilized zirconia (CSZ) remains stable at any temperatures (Etsell & Flengas, 1969; Subbarao & Maiti, 1984; Durrani *et al*., 2006). CSZ is frequently utilized as an oxygen sensor in metal refining process (Fray, 1996). In addition, ionic conductivity of CSZ has been studied and it can be used as a low-cost electrolyte of SOFC (Kurapova *et al*., 2017; Zhou & Ahmad, 2006; Muccillo *et al*., 2001). In the anode side, NiO is a prevalent anode material of SOFC because of high electrical conductivity and superior catalyst for H_2 oxidation. Merino *et al*. (2004) reported that NiO-CSZ cermet can be an alternatively suitable material for anode. The cermet has a sufficient electrical conductivity and a robust structure when the cermet is reduced.

Meanwhile in the cathode part, lanthanum and strontium-based composites such as lanthanum strontium manganite (LSM) are regularly used as cathode because of high oxygen reduction kinetics and electrical conductivity at 800-1,000 °C. However, this material is costly and only can operate in high temperatures. Besides, the barrier layer is needed because lanthanum- and strontium-based cathodes can react with zirconia-based electrolyte at 800-1,000 °C to form a low conductivity product such as $SrZrO_3$ and $La_2Zr_2O_7$ (Kindermann *et al*., 1996; Chen *et al*., 2014). $Ca_3Co_2O_6$ (CCO) recently emerged as a promising material for IT-SOFC cathode as it demonstrates good oxygen-reduction activity, relatively high electrical conductivity, good chemical stability up to 1300K, suitable thermal expansion with the electrolyte and thermoelectric capabilities for converting waste heat to electricity (Wei *et al*., 2013; Yu *et al*., 2017; Yu *et al*., 2015). In another study, Zn doping in CCO cathode leads to a reduced amount of cobalt and an increase in thermoelectric properties. The resistivity of $Ca_3Co_{2-x}Zn_xO_6$ (CCZO) lowers with increasing temperature and when the value of x is 0.1 (Takami & Ikuta, 2005). Therefore, CCZO can be a promising cathode of IT-SOFC.

In our previous study, we fabricated the anode-supported IT-SOFC cell consisting of NiO-CSZ anode as support, thin-film CSZ electrolyte, and CCZO-CSZ cathode. However, the physical characteristic and cell performance were exceedingly low because the electrolyte was too porous and the structure of anode easily fractured (Widiatmoko *et al*., 2019). In this work, we demonstrated an improvement to our previous study by fabricating an electrolyte-supported IT-SOFC single cell composed of CSZ electrolyte produced through dry pressing method, NiO-CSZ anode, and CCZO cathode fabricated by brush coating technique to obtain solid structure and improved electrochemical performance. The porosity of anode, density and hardness of electrolyte and morphology of each component were investigated. The electrolyte-supported cell was examined using hydrogen as fuel and ambient air as an oxidant at various operating temperatures. This paper serves a fundamental knowledge of the production and characterization of low-cost SOFC to boost the development and commercialization of SOFC technologies.

2. Materials and Methods

2.1 Cell Fabrication

Three wt% of CaO and 97 wt% of ZrO_2 acquired from Pingxiang Ball-Tec New Materials Co., Ltd (technical grade, Jianxi, China) were prepared by mixing with ethanol as a medium in a ball mill for 12 h at 90 rpm. The mixtures were dried at 100 °C for 24 h to produce CSZ powders. After drying, CSZ powder was pressed through dry pressing method at 10.5 MPa for 2.5 min to fabricate a disk-planar electrolyte-supported IT-SOFC. The CSZ pellet had a diameter of 37 mm and a thickness of 1 mm. The CSZ pellet was sintered at 1,480 °C for 2 h. On the other hand, 65 wt% of NiO purchased from Changsha Easchem Co., Ltd (technical grade, Changsa, China) and 35 wt% of CSZ were ball milled for 12 h at 90 rpm with ethanol as medium and 10 wt% of corn starch as pore former. Then, CaO, Co_3O_4 and ZnO, weighed in a stoichiometric amount, were blended with ethanol as medium and 1 wt% of polyethylene glycol (PEG) as a plasticizer from Bratachem (technical grade, Bandung, Indonesia) in a ball mill for 12 h at 90 rpm. Each electrode mixture was dried in an oven at 100 °C for 24 h to produce NiO-CSZ anode and $Ca_3Co_{1.9}Zn_{0.1}O_6$ (CCZO) cathode powders. To obtain anode and cathode slurries, each electrode powders were mixed with polyvinyl alcohol (PVA) as a binder and ethanol in a mass ratio of 1:0.1:10. Each mixture was dispersed homogenously using an ultrasonic bath for 30 min. The electrodes were painted onto both surfaces of CSZ electrolyte using a brush coating technique with an effective area of 1 cm^2. The NiO-CSZ anode and CCZO cathode were co-sintered at 1,100 °C for 3 h.

2.2 Physical Characterization

A scanning electron microscope (SEM, Hitachi SU3500, Hitachi High-Technologies Corporation, Tokyo, Japan) was used to observe the microstructure and the actual thickness of the cells. Prior to SEM examination, the single cell was coated with a thin film of gold in a sputtering system to prevent localized electric charging during imaging. JSM IT-300 (Jeol Ltd, Tokyo, Japan) Energy Dispersive X-Ray Spectroscopy (EDS) was used to define elemental composition in the area. The phase structure of CSZ was analyzed using X-Ray Diffractometer (XRD, Bruker D8 Advance, Karlsruhe, Germany) with Cu Kα radiation (λ = 1.5406 Å) with scanning angle from 0 to 100° (2θ) at a step size of 0.019°. Additionally, the density of CSZ pellets was evaluated using the Archimedes method with deionized water as the immersion medium, and the porosity of the anode was performed using ASTM C373-88. The hardness of CSZ electrolytes was obtained by Mohs method using SNI 7275-2008 in Center for Ceramics, Indonesia.

2.3 Electrochemical Characterization

An electrolyte-supported cell was located between two stainless steel (SS) 316L frame and sealed with ceramic paper and castable refractory cement C-18. A current collector in anode and cathode part was SS 304 mesh. In anode, NiO was reduced to Ni in situ at 800 °C with pure hydrogen in a tubular furnace.

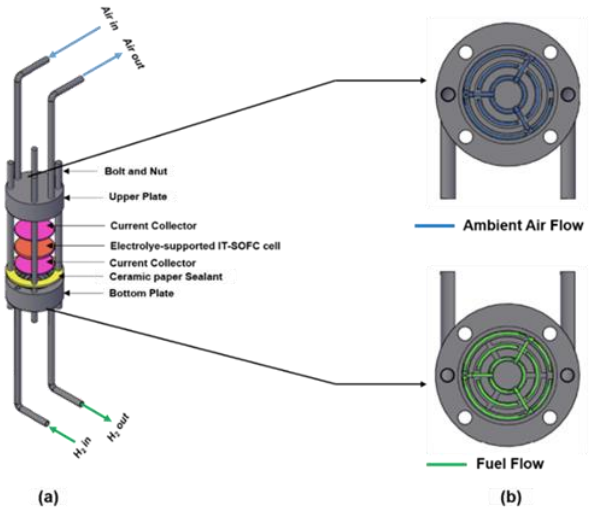

Fig. 1 (a) Schematic of an electrolyte-supported IT-SOFC cell testing (b) air (bottom view) and fuel (top view) flow path.

The sample was tested at 600, 700 and 800 °C using dry hydrogen and ambient air with a flow rate of 200 and 1,000 ml/min, respectively. The impedance cell was recorded from 100 kHz to 0.1 Hz under an open-circuit voltage (OCV) condition with AC amplitude of 10 mV and evaluated by using the equivalent circuit. Current-voltage characteristics and impedance at each temperature were carried out by Gamry V3000 potentiostat (Gamry Instruments, Warminster, USA). Figure 1 shows a schematic of cell testing to analyze the performance of an electrolyte-supported cell.

3. Result and Discussion

3.1 Physical Characteristic

The XRD result of CSZ electrolyte is presented in Figure 2. The spectra in Figure 2a indicated that a zirconia powder was dominated by monoclinic phase. A CSZ electrolyte was composed of the cubic, tetragonal and monoclinic phases as shown in Figure 2b. The 2θ of monoclinic peaks at 28.5° (111) and 31.8° ($\bar{1}11$) had higher intensity than other monoclinic peaks. Moreover, the intensity of other cubic orientations was lower than that of cubic (111) of 2θ peaks at around 30°. In addition, the monoclinic and cubic volume fraction (Vm and Vc) were calculated using Eq. (1) and (2) from the XRD peaks (Hermawan *et al*., 2017; Toraya *et al*., 1984).

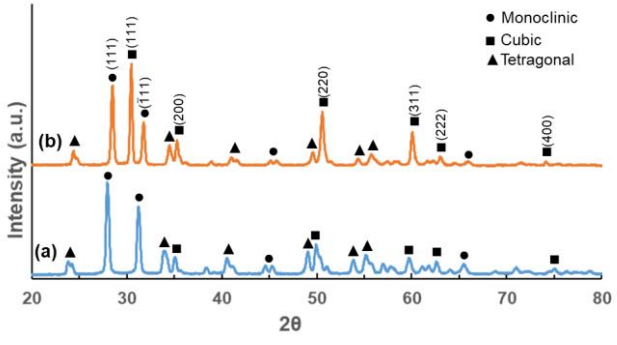

Fig 2. XRD patterns of (a) zirconia powder (b) CSZ electrolyte sintered at 1480 °C

$$V_m = \frac{1.115\, X_m}{1+0.115\, X_m},\ V_c = 1 - V_m \quad (1)$$

$$X_m = \frac{I_m(111) + I_m(\bar{1}11)}{I_m(111) + I_m(\bar{1}11) + I_c(111)} \quad (2)$$

$$\lambda = 2\,\frac{a}{\sqrt{3}}\,\sin\theta \quad (3)$$

Im and Ic data, the intensity of monoclinic [(111) and ($\bar{1}11$)] and cubic (111), are required to calculate the monoclinic peak intensity ratio called Xm. The value of Vm was 55.14% which implied the domination of monoclinic over cubic phase due to the low amount of calcia and low sintering temperature (Changlian *et al*., 2009). Moreover, the lattice parameter of CSZ electrolyte was estimated using Eq. (3), where λ is the x-ray wavelength (1.5406 Å), θ is the angle of cubic (111) phase and a is the lattice parameter (Å). The value of CSZ lattice parameter was 5.0724 Å. The lattice space of CSZ in this study was narrower than that of CSZ reported by Changlian *et al*. (2009) inasmuch as amount of calcia in this study (3 wt% of calcia) was lower than Changlian's work that used a 7 wt% of calcia loading. Besides the amount of calcia, the sintering temperature enhanced the lattice parameter since the formation of CSZ lattice required energy to diffuse more Ca^{2+} into zirconia lattice (Chourashiya, *et al*., 2008; Changlian, *et al*., 2009). The XRD results are fit with ICDD cards (ZrO_2; 01-083-0939 and $Ca_{0.2}Zr_{0.8}O_{1.8}$; 01-075-0359)

For cell dimension, the diameter of CSZ shrank from 37 to ~28 mm after sintering process. The relative density of sample sintered at 1,480 °C was approximately 83.3%. The low relative density was caused by a low amount of calcia. Changlian *et al*. (2009) reported that a CSZ pellet with 7 wt% of calcia sintered at 1,450 °C produced relative density of 94.5%, which is higher than that of CSZ with 3 wt% of calcia. Moreover, the hardness of CSZ electrolyte in Mohs' scale was 6, equal to 8.01 GPa which was slightly lower than that of commercial 8YSZ electrolyte (Dudek *et al*., 2011). The porosity of NiO-CSZ with 10 wt% of corn starch was about 23% before reduction. The 10 wt% of corn starch produced the optimum porosity of anode before and after reduction based on a study by Yoshito *et al*. (2009). SEM observation of cross-section and surface of NiO-CSZ/CSZ/CCZO-CSZ cell before test is shown in Figure 3. The traversed-section SEM structure of single cell was shown in Figure 3a. The microstructure of CSZ electrolyte was slightly porous as revealed in Figure 3b which confirmed a low relative density.

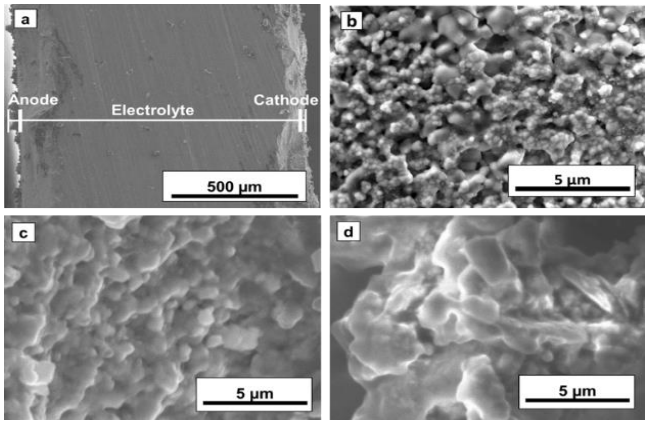

Fig. 3 SEM micrograph of (a) cross-section of an electrolyte-supported IT-SOFC cell; close view of (b) CSZ electrolyte; (c) NiO-CSZ anode and (d) CCZO cathode surface before testing

The sintering temperature was responsible to a quite porous microstructure in the CSZ electrolyte. At this temperature, the integration of grains was observed but they did not fully fill up the porosity of CSZ surface so that pinhole still existed. Moreover, the thickness of electrolyte was ~1 mm as shown in Figure 3a. The micrograph also confirmed that the NiO-CSZ anode and CCZO-CSZ cathode had a porous structure as revealed in Figure 3c and 3d. The thickness of anode and cathode was ~26.3 and ~42.4 µm, respectively. However, the layer of anode and cathode was not uniform.

3.2 Electrochemical Performance

I-V-P curves under different operating temperatures are reported in Figure 4a. OCV value of the single cell at 600, 700 and 800 °C was 0.43; 0.48; and 0.45 V, respectively. The measured OCV were lower than the theoretical OCV based on the Nernst equation. Fuel and oxidant crossover and gas leakage through ceramic paper and castable cement sealing to the environment were the main factors of significant distinction between experimental and theoretical OCV (Rasmussen *et al.*, 2008; Pusz *et al.*, 2007). Kim *et al.* (2019) reported that the presence of N_2 from the air in anode chamber can lower the OCV. The sinusoidal curves in Figure 4a show that peak power density at 600, 700 and 800 °C was 0.14; 0.50; and 1.00 mW/cm^2, respectively. The peak power density enhanced by approximately 500 times higher than our previous work based on anode-supported cell design at 700 °C (Widiatmoko *et al.*, 2019). However, the obtained result was extremely lower than other researches that used commercial YSZ-based msterials (Saebea, *et al.*, 2017). The contribution of ohmic and polarization resistances was exhibited by electrochemical impedance spectroscopy (EIS) analysis.

The spectra were matched with the circuit model as shown in Figure 4b. Rohm is the ohmic resistance of electrolyte, anode, cathode and current collector. The ohmic resistance was connected in series with two parallel R (resistance) and Q (constant phase element). The polarization resistance (Rp) consists of R1 indicating fast processes such as electronic and ionic charge transfer and R2 revealing slow processes such as diffusion and mass transfer (Li *et al.*, 2016; Leonide *et al.*, 2007).

The Rohm and Rp were summarized in Table 1. The Rohm values of 81.5 and 33.00 Ω were achieved at 700 and 800 °C, respectively. Thick electrolyte was responsible to high ohmic resistance in the cell (Park *et al.*, 2018; Tiwari & Basu, 2014). SS 304 current collector also contributed to increasing the ohmic resistance as the conductivity of SS 304 is much lower than Pt mesh/wire and the SS 304 mesh is easily oxidized at high temperature. SS 304 contains 18-20 wt% of Cr that can be evaporated and then form Cr deposit which poisons the electrodes and electrolyte. Figure 5 showed the cross-sectional EDS mapping of Ni, Co, Cr, Zn and O in the cell after examination. Ni was spread evenly at the top layer while Co and Zn were not clearly seen at the bottom layer due to extremely thin and not uniform layer. Cr was detected in electrodes and electrolyte with amount of 0.61 wt%. The presence of Cr from SS 304 in the precursor can lower the performance of the SOFC cell (Molin *et al.*, 2009; Zhou *et al.*, 2020; Jiang & Chen, 2014).

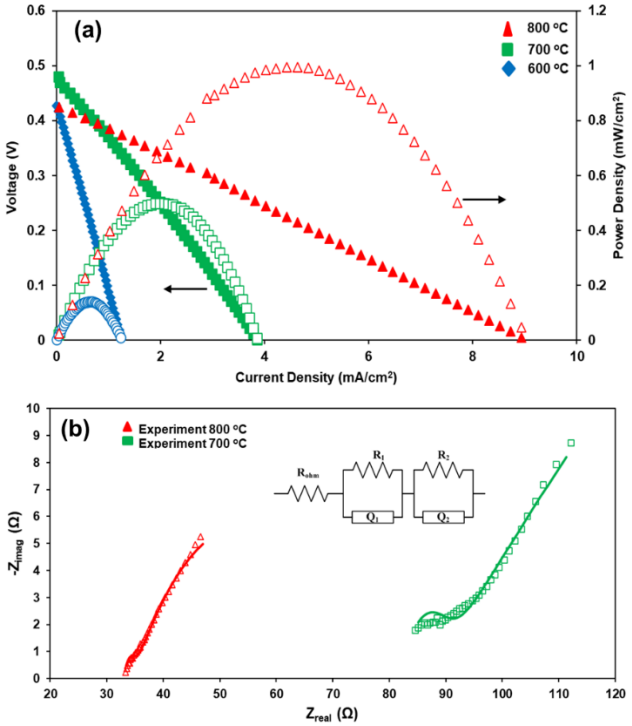

Fig. 4 (a) The I-V-P curves and (b) The Nyquist plot of NiO-CSZ/CSZ/CCZO-CSZ with H_2 flow rate of 200 ml/min and ambient airflow rates of 1,000 ml/min

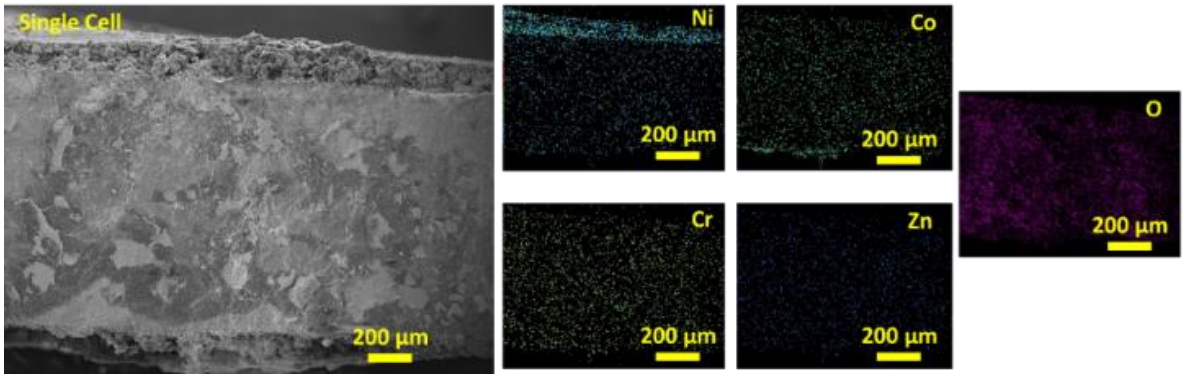

Fig. 5 EDS mapping of Ni, Co, Cr, Zn and O on the cross sectioned cell after test

Table 1
The resistance values extracted from an equivalent circuit of the Nyquist curves at 700 and 800 °C

T (°C)	R_{ohm} (Ω)	$R_p = R_1+R_2$ (Ω)	R_1 (Ω)	R_2 (Ω)
700	81.5	285.4	6.57	278.8
800	33.0	39.4	1.57	37.8

The polarization resistances at 700 and 800°C were 285.4 and 39.4 Ω, respectively. The high value of Rp was related to conductivity and mass transfer in anode and cathode. The electrical conductivity of the electrodes, NiO-CSZ anode and CCZO cathode, are slightly lower than conventional electrodes of SOFC (Ouri *et al*., 2015; Paydar *et al*., 2016).

4. Conclusion

In this work, an electrolyte-supported IT-SOFC cell with low-cost material was successfully fabricated and evaluated. The single cell contained NiO anode, CSZ electrolyte, and CCZO cathode. The structure of electrodes was porous while the electrolyte had a quite porous morphology which was potential for gas crossover phenomenon. The electrochemical characterization exhibited ~500 times increase in the maximum power density at 700°C from our previous research. Nevertheless, the voltage and power density were still low compared to YSZ-based IT-SOFC. In future work, the improvement of low-cost electrolyte fabrication is a critical part to prevent fuel and oxidant crossover. Additionally, a gas-tight sealing material is needed to avoid gas leakage into the environment.

Acknowledgments

This work was funded by the International R&D Academy of Korean Institute of Science and Technology (KIST) [Grant number 19-7887].

Conflicts of Interest: The authors declare no conflict of interest.

References

Abdalla A.M., Hossain, S., Azad A.T., Petra, P.M.I., Begum, F., Eriksson, S.G. & Azad, A.K. (2018) Nanomaterials for solid oxide fuel cells: A review. *Renewable & Sustainable Energy Reviews*, 82, pp. 353–368; doi: 10.1016/j.rser.2017.09.046.

Changlian, C., Qiang, S., Junguo, L. & Lianmeng, Z. (2009) Sintering and phase transformation of 7wt% calcia-stabilized zirconia ceramics. *Journal of Wuhan University Technology-Mater. Sci. Ed*, 24, 304–307. doi: 10.1007/s11595-009-2304-0.

Chelmehsara, M.E. & Mahmoudimehr, J. (2018) Techno-economic comparison of anode-supported, cathode-supported, and electrolyte-supported SOFCs. *International Journal of Hydrogen Energy*, 43(32), 15521-15530. doi: 10.1016/j.ijhydene.2018.06.114.

Chen, Y., Yang, L., Ren, F. & An, K. (2014) Visualizing the structural evolution of LSM/xYSZ composite cathodes for SOFC by in-situ neutron diffraction. *Scientific Reports*, 1-9. doi: 10.1038/srep05179.

Chourashiya, M.G., Patil, J.Y., Pawar, S.H. & Jadhav, L.D. (2008). Studies on structural, morphological and electrical properties of $Ce_{1-x}Gd_xO_{2-(x/2)}$. *Materials Chemistry and Physics*, 109, 39-44. doi: 10.1016/j.matchemphys.2007.10.028.

Dudek, M., Mosiałek, M., Mordarski, G., Socha, R. & Rapacz-Kmita, A.. (2011) Ionic Conductivity of the CeO_2-Gd_2O_3-SrO System. *Archives of Metallurgy and Materials*, 56, 2874–2889. doi: 10.2478/v10172-011-0143-4.

Durrani, S.K., Akhtar, J., Ahmad, M. & Hussain, M.A. (2006) Synthesis and characterization of low density calcia stabilized zirconia ceramic for high temperature furnace application. *Materials Chemistry and Physic*, 100, 324–328. doi: 10.1016/j.matchemphys.2006.01.010.

Etsell, T. & Flengas, S. (1969) The electrical properties of solid oxide electrolytes. *Chemical Reviews*, 70, 339–376. doi: 10.1021/cr60265a003.

Fleischhauer, F., Bermejo, R., Danzer, R., Mai, A., Graule, T. & Kuebler J. (2015) Strength of an electrolyte supported solid oxide fuel cell. *Journal of Power Sources*, 297, 158–167. doi: 10.1016/j.jpowsour.2015.07.075.

Fragiacomo, P., De Lorenzo, G. & Corigliano, O. (2020) Intermediate temperature solid oxide fuel cell/electrolyzer towards future large-scale production. *Procedia Manufacturing*, 42, 259-266. doi: 10.1016/j.promfg.2020.02.082.

Fray, D.J. (1996) The use of solid electrolytes as sensors for applications in molten metals. *Solid State Ionics*, 86–88, 1045–1054. doi: 10.1016/0167-2738(96)00249-4.

Hermawan, E., Lee, G.S., Kim, G.S., Ham H.C., Han, J. & Yoon S.P. (2017) Densification of an YSZ electrolyte layer prepared by chemical/electrochemical vapor deposition for metal-supported solid oxide fuel cells, *Ceramics International*, 43,10450–10459. doi: 10.1016/j.ceramint.2017.05.085.

Irshad, M., Siraj, K., Raza, R., Ali, A., Tiwari, P., Zhu, B., Rafique, A., Ali, A., Ullah, M.K. & Usman, A. (2016) A brief description of high temperature solid oxide fuel cell's operation, materials, design, fabrication technologies and performance. *Applied Sciences*, 6(3), 1-23. doi: 10.3390/app6030075.

Jiang, S.P. & Chen, X. (2014) Chromium deposition and poisoning of cathodes of solid oxide fuel cells: A review. *International Journal of Hydrogen Energy*, 39, 505-531. doi: 10.1016/j.ijhydene.2013.10.042.

Kim, G.S., Lee, B.Y., Accardo, G., Ham, H.C., Moon, J. & Yoon, S.P. (2019) Improved catalytic activity under internal reforming solid oxide fuel cell over new rhodium-doped perovskite catalyst. *Journal of Power Sources*, 423, pp. 305–315. doi: 10.1016/j.jpowsour.2019.03.082.

Kindermann, L., Das, D., Nickel, H. & Hilpert, K. (1996) Chemical compatibility of the LaFeO3 base perovskites $(La_{0.6}Sr_{0.4})_zFe_{0.8}M_{0.2}O_{3-\delta}$ (z = 1, 0.9; M = Cr, Mn, Co, Ni) with yttria stabilized zirconia. *Solid State Ionics*, 89, 215–220. doi: 10.1016/0167-2738(96)00366-9.

Kurapova, O.Y., Glumov, O.V., Pivovarov, M.M &, Golubev, S.N. (2017) Structure and Conductivity of Calcia Stabilized Zirconia Ceramics, Manufactured from Freeze-Dried Nanopowder. *Reviews on Advanced Materials Science*, 52, 134–141. doi: 10.1515/rams-2018-0071.

Leonide, A., Sonn, V., Weber, A. & Ivers-Tiffée, E. (2007) Evaluation and Modeling of the Cell Resistance in Anode-Supported Solid Oxide Fuel Cells. *Journal of Electrochemical Society*, 155, 36-41. doi: 10.1149/1.2801372

Li, Y., Wang, S. & Su, P. (2016) Proton-conducting Micro-solid Oxide Fuel Cells with Improved Cathode Reactions by a Nanoscale Thin Film Gadolinium-doped Ceria Interlayer. *Scientific Reports*, 6, 1–9. doi: 10.1038/srep22369.

Merino, R.I., Pena, J.I., Laguna-Bercero, M.A., Larrea, A. & Orera, V.M. (2004) Directionally solidified calcia stabilized zirconia-nickel oxide plates in anode supported solid oxide fuel cells. *Journal of the European Ceramic Society*, 24, pp. 1349-1353. doi: 10.1016/S0955-2219(03)00562-4.

Molin, S., Gazda, M. & Jasinski, P. (2009) Interaction of yttria stabilized zirconia electrolyte with Fe_2O_3 and Cr_2O_3. *Journal of Power Sources*, 194, 20-24. doi: 10.1016/j.jpowsour.2009.01.03

Muccillo, R., Netto, R.C. & Muccillo, E.N. (2001) Synthesis and characterization of calcia fully stabilized zirconia solid electrolytes. *Material Letters*, 49, 197–201. doi: 10.1016/S0167-577X(00)00367-0

Orui, H., Nozawa, K., Arai, H. & Kanno, R. (2015) Influence of reduction conditions on electrical properties of NiO-Zirconia

composites for solid oxide fuel cell electrode. *Journal of Power Sources*, 288, 419-425. doi: 10.1016/j.jpowsour.2015.04.139

Park, J.M., Kim, D.Y., Baek, J.D., Yoon, Y.J., Su, P.C. & Lee, S.H. (2018) Effect of electrolyte thickness on electrochemical reactions and thermo-fluidic characteristics inside a SOFC unit cell. *Energies*, 11(473), 1-25. doi: 10.3390/en11030473.

Paydar, S., Shariat, M.H. & Javadpour, S. (2016) Investigation on electrical conductivity of LSM/YSZ8, LSM/$Ce_{0.84}Y_{0.16}O_{0.96}$ and LSM/$Ce_{0.42}Zr_{0.42}Y_{0.16}O_{0.96}$ composite cathodes of SOFCs. *International Journal of Hydrogen Energy*, 41, 23145-23155. doi: 10.1016/j.ijhydene.2016.10.092.

Pusz, J., Smirnova, A., Mohammadi, A. & Sammes, N.M. (2007) Fracture strength of micro-tubular solid oxide fuel cell anode in redox cycling experiments. *Journal of Power Sources*, 163, 900–906. doi: 10.1016/j.jpowsour.2006.09.074.

Rasmussen, J.F.B., Hendriksen, P.V. & Hagen, A. (2008) Study of Internal and External Leaks in Tests of Anode-Supported SOFCs. *Fuel Cells*, 8, 385–393. doi: 10.1002/fuce.200800019.

Saebea, D., Authayanun, S., Patcharavorachot, Y., Chatrattanawet, N. & Arpornwichanop, A. (2018) Electrochemical performance assessment of lowtemperature solid oxide fuel cell with YSZ-based and SDC-based electrolytes. *International Journal of Hydrogen Energy*, 43, 921-931. doi: 10.1016/j.ijhydene.2017.09.173.

Shi, H., Su, C., Ran, R., Cao, J. & Shao, Z. (2020) Electrolyte materials for intermediate-temperature solid oxide fuel cells. *Progress in Natural Science: Materials International*, 30, 764-774. doi: 10.1016/j.pnsc.2020.09.003.

Singhal, S.C. & Kendall, K. (2003) High-temperature Solid Oxide Fuel Cells: Fundamentals, Design and Applications, Oxford: Elsevier Ltd.

Subbarao, E. & Maiti, H. (1984) Solid Electrolyte with Oxygen Ion Conduction. *Solid State Ionics*, 11, 317–338. doi: 10.1016/0167-2738(84)90024-9.

Takami, T. & Ikuta, H. (2005) Thermoelectric properties of one-dimensional cobalt oxide $Ca_3Co_2O_6$ and the effect of Zn doping, *24th International Conference on Thermoelectrics*, 480-483. doi: 10.1109/ICT.2005.1519990.

Timurkutluk, B., Timurkutluk, C., Mat, M.D. & Kaplan, Y. (2016) A review on cell/stack designs for high performance solid oxide fuel cells. *Renewable & Sustainable Energy Reviews*, 56, 1101–1121. doi: 10.1016/j.rser.2015.12.034.

Tiwari, P. & Basu, S. (2014) Performance studies of electrolyte-supported solid oxide fuel cell with Ni-YSZ and Ni-TiO2-YSZ as anodes. *Journal of Solid State Electrochemistry*, 18, 805–812. doi: 10.1007/s10008-013-2326-6.

Toraya, H., Yoshimura, M. & Somiya, S. (1984) Quantitative Analysis of Monoclinic-Stabilized Cubic ZrO2 Systems by X-Ray Diffraction. *Journal of the American Ceramic Society*, 67, 183-184. doi: 10.1111/j.1151-2916.1984.tb19614.x.

U.S. Geological Survey. (2019) Mineral commodity summaries 2019, U.S. Geological Survey, Virginia, Feb. 2019.

Wei, T., Huang, Y.H., Zeng, R., Yuan, L.X., Hu, X.L, Zhang WX., Jiang, L., Yang, J.Y. & Zhang, Z.L. (2013) Evaluation of Ca3Co2O6 as cathode material for high-performance solid-oxide fuel cell. *Scientific Reports*, 3, 1–6. doi: 10.1038/srep01125.

Widiatmoko, P., Devianto, H., Nurdin, I., Yusupandi, F., Kevino. & Ovani, E.N. (2019) Fabrication and characterization of intermediate-temperature solid oxide fuel cell (IT-SOFC) single cell using Indonesia's resources. *IOP Conference Series: Material Science and Engineering*, 550. doi: 10.1088/1757-899X/550/1/012001.

Yoshito, W.K., Matos, J.R., Ussui, V., Lazar, D.R.R. & Paschoal, J.O.A. (2009) Reduction kinetics of NiO-YSZ composite for application in solid oxide fuel cell. *Journal of Thermal Analysis and Calorimetry*, 97, 303–308. doi: 10.1007/s10973-009-0237-7.

Yu, S., He, S., Chen, H. & Guo, L. (2015) Effect of calcination temperature on oxidation state of cobalt in calcium cobaltite and relevant performance as intermediate- temperature solid oxide fuel cell cathodes. *Journal of Power Sources*, 280, 581–587. doi: 10.1016/j.jpowsour.2015.01.150.

Yu, S., Zhang, G., Chen, H. & Guo, L. (2017) A novel post-treatment to calcium cobaltite cathode for solid oxide fuel cells. *International Journal of Hydrogen Energy*, 43, 2436-2442. doi: 10.1016/j.ijhydene.2017.12.040.

Zhang, K., Kleit, A.N. & Nieto, A. (2017) An economics strategy for criticality – Application to rare earth element yttrium in new lighting technology and its sustainable availability. *Renewable & Sustainable Energy Reviews*, 77, 899-915. doi: 10.1016/j.rser.2016.12.127.

Zhou, L., Mason, J.H., Li, W. & Liu, X. (2020) Comprehensive review of chromium deposition and poisoning of solid oxide fuel cells (SOFCs) cathode materials. *Renewable & Sustainable Energy Reviews*, 134, 110320-110343. doi: 10.1016/j.rser.2020.110320.

Zhou, M. & Ahmad, A. (2006) Synthesis, processing and characterization of calcia-stabilized zirconia solid electrolytes for oxygen sensing applications. *Materials Research Bulletin*, 41, 690–696. doi: 10.1016/j.materresbull.2005.10.018